

Observed Vertical Structure of Tropical Clouds Sorted in Large-scale Regimes

Hui Su, Jonathan H. Jiang, Deborah G. Vane

Jet Propulsion Laboratory, California Institute of Technology, Pasadena, CA, 91109 USA

Graeme L. Stephens

Department of Atmospheric Science, Colorado State University, Fort Collins, CO,
80523, USA

Hui Su, M/S 183-701, Jet Propulsion Laboratory, California Institute of Technology, 4800 Oak Grove Drive, Pasadena, California 91109-8099, U.S.A.

(email: Hui.Su@jpl.nasa.gov)

1 **Abstract.** The CloudSat cloud water content (CWC) profiles are sorted by a number of large-scale
2 parameters obtained from reanalysis and satellite observations, including 500 hPa vertical
3 velocity, sea surface temperature and its gradient, surface divergence, precipitation, water vapor
4 path, convective available potential energy and lower tropospheric static stability. The sorting is
5 physics-based and phenomenon-oriented. We find different degrees of clustering of cloud vertical
6 structure in various large-scale regimes. The dominant modes are the deep and shallow clouds
7 with peak CWC above 7 km and below 2 km, respectively, corresponding to distinctly different
8 large-scale regimes. A middle-level peak of CWC around 5-7 km is discernible associated with
9 the large-scale conditions similar to the shallow clouds. This study provides the first quantitative
10 and comprehensive view of tropical CWC distributions in large-scale regimes. These results offer
11 insights into cloud parameterizations and serve as new observational metrics for evaluation of
12 cloud simulations in models.

1 1. Introduction

2 Tropical cloud structure is closely related to the ambient large-scale dynamic and
3 thermodynamic conditions. Emanuel [1994, *Figure 14.7*] showed that the transition of shallow
4 clouds into deep clouds is associated with the warming of sea surface temperature (SST) and the
5 change of large-scale descending regime into ascending regime. However, this general picture of
6 cloud structure as a function of large-scale regimes needs observational quantification for cloud
7 parameterizations and evaluation of cloud simulations in large-scale models. CloudSat, for the first
8 time, makes this quantification possible by providing a global survey of cloud profiles from space-
9 borne millimeter cloud profiling radar (CPR) since June 2006.

10 *Haynes and Stephens* [2007] analyzed CloudSat cloud mask profiles in relation to precipitation.
11 They found three cloud modes (deep, shallow and middle-level clouds) in the tropics, in line with
12 the trimodal structure of tropical convection found by *Johnson et al.* [1999]. It has also been
13 showed that different geographical regions exhibit different characteristics of cloud vertical
14 structure, in association with different dynamics [*Back and Bretherton*, 2006; *Kubar and*
15 *Hartmann*, 2008].

16 An increasingly popular method to identify the relations of clouds with large-scale dynamics is
17 to sort cloud profiles (and cloud radiative effects) by 500 hPa vertical velocity (ω_{500}). This sorting
18 technique is proved to be useful in understanding cloud variability and identifying differences
19 among models for cloud feedback estimates [e.g. *Bony et al.*, 2004; *Wyant et al.*, 2006]. *Zhang et*
20 *al.* [2007] performed the “cluster analysis” on the vertical profiles of CloudSat radar reflectivity
21 and sorted the occurrence frequency of each cloud cluster by NCEP ω_{500} . They stressed that the
22 dynamics sorting technique is important for model-data comparisons.

1 In this paper, we analyze 1-year (January to December 2007) of cloud water content (CWC)
2 profiles from the CloudSat Level 2B Cloud Water Content Radar-Only product and sort them by a
3 number of large-scale parameters. The CWC is the sum of cloud liquid water content (LWC) and
4 ice water content (IWC), both of which are usually direct model output variables and inputs to
5 radiation calculations. Hence, analysis of these two observed quantities provides a direct reference
6 for evaluation of simulated cloud amount and associated cloud radiative effects. The large-scale
7 parameters we use here include not only ω_{500} , but also SST, surface convergence, SST gradient,
8 precipitation, column-integrated water vapor path (WVP), convective available potential energy
9 (CAPE), and lower tropospheric stability (LTS, defined as the potential temperature difference
10 between 700 hPa and surface, as in *Klein and Hartmann* [1993]). Except ω_{500} , all other parameters
11 are obtained or derived from satellite observations. The choice of these parameters is based on the
12 existing knowledge of their connection with convection; yet a quantitative view of the observed
13 CWC distributions in each large-scale regime is not known. We present the results in terms of the
14 annual averages for Year 2007. The seasonal and day-night differences are discussed. A forth-
15 coming paper will focus on the comparison of the observed regime-specific cloud structure with a
16 few state-of-the-art general circulation models (GCMs).

17 2. Data and Methodology

18 CloudSat is a member of the A-train satellite constellation, with equatorial crossing time around
19 1:30 am and 1:30 pm. The horizontal resolution of CloudSat IWC and LWC is about 2.5 km along
20 track and 1.4 km cross track. The vertical resolution is about 240 m.

21 The collocation of large-scale parameters with the CloudSat measurements is greatly facilitated
22 by the A-train. The Advanced Microwave Scanning Radiometer (AMSR-E) on Aqua provides
23 nearly simultaneous SST and WVP measurements. We downloaded the twice-daily SST and WVP

1 data with a resolution of $0.25^{\circ} \times 0.25^{\circ}$ from the Remote Sensing Systems (<http://www.remss.com>).
 2 SST gradient is then calculated using the centered difference scheme. The Atmospheric Infrared
 3 Sounder (AIRS) on Aqua provides atmospheric temperature and water vapor profiles. From its
 4 Level 3 product (with a horizontal resolution of $1^{\circ} \times 1^{\circ}$) we calculated CAPE and LST. We assume
 5 an air parcel is lifted pseudo-adiabatically from 1000 hPa when calculating CAPE.

6 Precipitation is from the Tropical Rainfall Measuring Mission (TRMM). We use the 3B42 3-
 7 hourly product with a resolution of $0.25^{\circ} \times 0.25^{\circ}$, which combines the rainfall estimates from radar,
 8 infrared and microwave instruments and rain gauges. We derive surface convergence using surface
 9 wind measurements from the Quick Scatterometer (QuikSCAT) and compare it with that
 10 calculated from the NCEP surface winds. The results are very similar as NCEP assimilates
 11 QuikSCAT winds in its analysis. As QuikSCAT orbits have large offsets from the CloudSat orbits
 12 in both time and space, we decided to use NCEP 6-hourly surface wind divergence instead of
 13 QuikSCAT to ensure maximum overlapping of CloudSat CWC with the surface divergence field.
 14 The ω_{500} is from NCEP, with a horizontal resolution of $2.5^{\circ} \times 2.5^{\circ}$.

15 All large-scale variables are interpolated onto the CloudSat tracks in both space and time. For
 16 each large-scale variable, 25 bins are specified. Then the CWC profiles within each bin are
 17 averaged. Only tropical (30°S - 30°N) oceanic measurements are considered in the binning. We
 18 used ~36 million IWC and LWC profiles for the one-year data analysis (over 2 terabytes in size).

19 **3. Geographical distributions of cloud profiles**

20 Figure 1a shows the tropical-mean IWC, LWC and CWC profiles observed by CloudSat
 21 averaged for 2007 and Figure 1b shows the zonal mean CWC at all latitudes. The tropical-mean
 22 CWC profile exhibits a double-peak structure: one at ~1.5 km and the other at ~7 km. The
 23 transition of liquid clouds into ice clouds occurs between 5 km to 9 km (the freezing layer) in the

1 tropical-mean. The amplitude of IWC is much smaller than LWC. In the tropics, the strongest
 2 zonal-mean CWC is within 15 degrees of the equator in the lower troposphere, with higher values
 3 in the northern hemisphere than in the southern hemisphere. Accordingly, the minimum LWC is in
 4 the northern hemisphere around 20°N. Zonal-mean IWC is approximately symmetric about the
 5 equator. The maximum cloud top heights are over 17 km in the tropics and decrease poleward. In
 6 the mid-latitude storm tracks (50°-70°S/N), CWC reaches maximum intensity around 2-3 km.

7 Figure 2 shows the maps of annual mean CWC at four heights. Substantial differences exist at
 8 the four levels. At 2 km, large CWC (liquid only) occurs over the western Pacific (WP), the Indian
 9 Ocean (IN), south Pacific convergence zone (SPCZ), inter-tropical convergence zone (ITCZ),
 10 northern South America (SAM), equatorial Atlantic (EA) and extra-tropical storm tracks. At 5 km,
 11 CWC (mostly LWC plus small amount of IWC) decreases markedly in eastern Pacific (EP), EA,
 12 ITCZ, SPCZ and extra-tropics; but it is stronger than or as strong as that at 2 km over WP, IN and
 13 SAM. CWC (IWC only) at 9 km is large in WP, South Asia, IN, SAM and central Africa, while it
 14 is more confined above these convective centers at 16 km and smaller in magnitude than that at 9
 15 km by a factor of 20 or more.

16 **4. Tropical cloud profiles sorted by large-scale parameters**

17 Figure 3 displays the one-year CWC profiles sorted by eight coincident large-sale parameters
 18 over the tropical oceans. The probability density functions (PDF) of each large-scale parameter are
 19 superimposed. We leave out the bins within which the number of measurements is less than 150 (6
 20 orders of magnitude less than the total number of measurements). We also tried a variant of the
 21 display of the bin plots in which stretched x-axes in proportion to the PDF of the large-scale
 22 variables were used as in Wyant *et al.* [2006]. The resulting CWC patterns highlight the dominant
 23 cloud modes but hide away the infrequent modes (figure not shown). To faithfully represent all

1 possible observed cloud variabilities, we decided not to use the stretched x-axes. However, when
 2 comparing the observations with GCMs, using the stretched x-axes may be more useful. The
 3 horizontal maps of the annual-mean large-scale variables are also shown in Figure 3.

4 To characterize the CWC distributions in each large-scale regime, we broadly categorize the
 5 cloud structure by the height of local CWC maxima: below 2 km as the shallow clouds, 5-7 km as
 6 the middle clouds and above 7 km as the deep clouds, in rough correspondence to *Johnson et al.*
 7 [1999] and *Haynes and Stephens* [2007]. Note that deep convective clouds may bear double peaks
 8 in the CWC vertical profiles, one in the boundary layer and one in the upper levels. In this case, the
 9 low-level peak is not regarded as a separate “shallow” mode. As illustrated in Figure 3, the actual
 10 CWC profiles for each mode exhibit large variabilities in different large-scale regimes.

11 ω_{500}

12 The PDF of ω_{500} is approximately symmetric about the peak near zero (shifted slightly positive),
 13 dictated by the tropical mass balance (Figure 3a). Ascents coincide with deep convective regions,
 14 while descents are in EP and the subtropics. In the large-scale ascent regime, the CWC profiles are
 15 “deep” with large CWC from 5 km to 15 km and a secondary peak (LWC) below 2 km. As ω_{500}
 16 changes from negative to positive, LWC increases. In the subsidence regime, clouds are “shallow”
 17 with maximum CWC in the boundary layer. Over the strongest subsidence regions ($\omega_{500} > 0.4$
 18 Pa/s), cloud tops are capped below 3 km. The occurrence frequency of these clouds is about 6.3%.
 19 In Figure 3a, the middle-level clouds are not clear.

20 SST

21 The horizontal map of SST shows close association with ω_{500} : warm SST corresponds to ascents
 22 and cold SST corresponds to descents. However, the SST distribution is smoother than that of
 23 ω_{500} . Its PDF has a broad peak around 298-302 K. When sorted by SST, CWC exhibits three

1 modes: the deep mode with peak CWC higher than 7 km in the warm SST (> 300 K) regime, the
 2 shallow mode with maximum CWC below 2 km over the SST of ~ 288 -300 K, and an
 3 inconspicuous middle-level mode with peak CWC around 5-7 km overlying the shallow clouds
 4 (Figure 3b). The CWC magnitude for the middle clouds is 10 times smaller than the deep and
 5 shallow clouds. Over the coldest SST (< 290 K), the CWC profiles maximize in the high altitudes
 6 but the magnitudes are much weaker than the deep clouds over the warmer SST (> 300 K). The
 7 occurrence frequency of these clouds is only 0.01%. They may result from the intrusion of mid-
 8 latitude storms in the subtropics or cirrus detrainments from decayed convection.

9 **Surface divergence**

10 Deep convection is usually associated with convergent flow near the surface. Figure 3c
 11 illustrates the cloud structure in the domain of surface divergence. The pattern of surface
 12 divergence resembles that of ω_{500} , with peak occurrence near zero (shifted towards $1 \times 10^{-5} \text{ s}^{-1}$). The
 13 binned CWC shows the deep and shallow modes distinctly, and a weak but discernible middle
 14 mode. The deep mode is centered at surface convergence about $-2 \times 10^{-5} \text{ s}^{-1}$, with the high-level
 15 and low-level peaks of similar magnitudes. The shallow clouds are distributed over surface
 16 divergence from 0 to $2 \times 10^{-5} \text{ s}^{-1}$. The weak middle-level mode lies above the shallow mode, but
 17 more concentrated towards surface divergence of $2 \times 10^{-5} \text{ s}^{-1}$.

18 **SST gradient**

19 SST gradient is believed to be another important factor that determines tropical circulation and
 20 convection [Lindzen and Nigam, 1987]. In the tropics, the meridional SST gradient is much
 21 stronger than the zonal SST gradient and thus the magnitude of SST gradient shown in Figure 3h is
 22 dominated by the meridional SST gradient. Large SST gradients are observed in the equatorial EP,
 23 California and Peruvian coasts and subtropical oceans, mostly surface divergent regions. The PDF

1 of SST gradient shows a nearly monotonic decrease as gradient increases. The binned CWC
 2 profiles are rather different from the previous three. Although the deep mode is evident over the
 3 relatively weak SST gradient regime, the peak CWC in the upper levels is much weaker than the
 4 counterparts in Figure 3a-c. The high clouds are distributed quite evenly in the SST gradient
 5 domain, unlike the highly clustered structure in the domains of ω_{500} , SST and surface divergence.
 6 This suggests that the change of SST gradient only weakly affects the high cloud amount. The
 7 strongest CWC is distributed over the relatively weak SST gradient regime of 10×10^{-6} K/m, while
 8 the middle-level clouds are scattered over the large SST gradient between 30 to 40×10^{-6} K/m with
 9 very low occurrence frequency ($\sim 0.001\%$).

10 **Precipitation**

11 Defining the minimum rain rate for precipitating clouds being 0.001 mm/h, we find that the
 12 occurrence frequency of precipitation over the tropical oceans is about 14.5% (If the threshold rain
 13 rate is raised to 0.1 mm/h, the tropical precipitation occurrence would be $\sim 7\%$, in closer agreement
 14 with that in *Haynes and Stephens* [2007]). About 85% of precipitating clouds have surface rain
 15 rates less than 2 mm/h and they contribute to 45% of tropical rainfall. Only 15% of the
 16 precipitating clouds have rain rates greater than 2 mm/h but they constitute about 55% of the total
 17 rainfall. Shallow clouds are spread over the weak precipitation regime, where the middle-level
 18 clouds are also pervasive. In the heavy precipitation regime (> 2 mm/h), the deep clouds dominate.

19 **Water vapor path**

20 Atmospheric moisture is closely linked to cloud processes. The PDF of WVP has a broad peak
 21 from 20-50 mm and decreases sharply when WVP is greater than 50 mm. The moist air columns
 22 with WVP > 50 mm account for 0.3% of the total air columns, but they contain 57% of total
 23 precipitable water. Deep clouds are highly concentrated in the moist air columns and shallow

1 clouds are distributed over the drier environment. Over the moistest regime, CWC peaks strongly
2 in the upper levels with little liquid water below 5 km. There are hints of middle-level clouds
3 distributed above the shallow clouds in the drier air columns, but their CWC is quite small.

4 **Convective available potential energy**

5 The CAPE is proportional to the buoyancy of an air parcel when it is lifted. Convection tends to
6 consumes CAPE and restores atmosphere to neutral stability. Figure 3o shows the horizontal
7 distribution of annual-mean CAPE for the tropical oceans. The pattern is very similar to that of
8 precipitation and WVP, with the peak value around 1200 J/Kg over the deep convective regions.
9 The instantaneous CAPE values are much higher. Its PDF is a monotonically decreasing function.
10 The binned CWC profiles display certain degree of clustering: the shallow clouds occur over the
11 low CAPE (< 500 J/Kg) regions and the deep clouds are associated with higher CAPE (> 4000
12 J/kg). The middle-level clouds seem to be indistinguishable from the deep clouds in the CAPE
13 domain as the CWC contours spread quite continuously between ~ 6 km and ~ 13 km.

14 **Lower tropospheric stability**

15 The LTS is found highly correlated with the occurrence of stratiform clouds [*Klein and*
16 *Hartmann*, 1993]. The calculated LTS from AIRS is nearly a ‘complement’ to CAPE, in that high
17 CAPE corresponds to low LTS and vice versa (Figure 3p). The PDF of LTS peaks around 14 K
18 and skews to higher occurrence in large LTS than in small LTS. The shallow clouds are mostly
19 distributed over stable lower troposphere with $LTS > 14$ K, while the double-peaked deep mode is
20 concentrated over less stable lower troposphere where LTS is less than 10 K. In Figure 3i, a cluster
21 of middle to high clouds are noticeable over very high LTS values (> 25 K), overlapping above
22 strong LWC in the boundary layer. Their occurrence frequency is only 0.01%, though.

23 **5. Seasonal and day-night differences**

Besides the annual means, we also examined the seasonal and day-night differences for the regime-sorted cloud profiles. The overall characteristics of cloud clustering are consistent in all seasons (figure not shown). The major difference is the magnitudes of IWC and LWC. In general, the peak IWC for the deep clouds is larger in northern winter than in summer while the peak LWC for the stratiform clouds is larger in northern summer than in winter. Comparing the day-time and night-time CWC, IWC tends to be larger in the day, while LWC tends to be larger at night due to more efficient radiative cooling at night than in the day.

6. Conclusions

This study examines the CloudSat observed CWC profiles sorted in a number of large-scale regimes. We find that two distinct modes dominate the vertical structure of tropical clouds. The deep mode with the peak CWC around 8-10 km is associated with mid-tropospheric ascent, warm SST, surface convergence, weak SST gradient, heavy precipitation, moist air, large CAPE and weak lower-tropospheric static stability. The opposite conditions apply to the shallow clouds which have peak CWC (i.e., LWC) at 1-2 km. Although the deep and shallow modes are outstanding in all large-scale regimes, the actual CWC profiling for each mode varies in different large-scale parameter space. The linkage of the deep and shallow modes with their respective large-scale regimes is expected, but the quantification of the CWC amount in each regime is a break-through result. We also find an infrequent middle-level cloud mode. These middle-level clouds usually overlie above the shallow clouds with surface conditions that are not favorable to deep convection, i.e., cold SST, strong surface divergence, large SST gradient, dry air and stable lower troposphere. The hypothesis that these clouds may result from the influence of middle-latitude storms is largely ruled out when we find that the features for this mode are robust even when the binning averages are restricted to 15°S-15°N, despite of their very low occurrence

1 frequency (figures not shown). Therefore, we tend to think that these middle clouds may be
 2 associated with convection initiated at middle-levels. The physical processes that produce these
 3 middle clouds need to be further studied. Exploring more large-scale parameters such as middle
 4 tropospheric humidity, lapse rate and wind shear as “regime-identifiers” may help to elucidate
 5 their origins. A caveat of the CloudSat data is that the upper tropospheric thin cirrus is
 6 underestimated. Future work that combines CloudSat and Cloud Aerosol Lidar and Infrared
 7 Pathfinder Satellite Observations (CALIPSO) measurements would provide a more complete
 8 representation of the tropical cloud structure.

9 Although the association of cloud structure with large-scale dynamics has been established for a
 10 long time, the lack of observed CWC profiles in connection with large-scale regimes hindered the
 11 evaluation of cloud simulations and improvement of cloud parameterizations in climate models.
 12 The regime-sorted cloud profiles presented in this paper can serve as new observational metrics
 13 for comparison with models. Because they are physics-based and phenomenon-oriented, using
 14 them as model-data comparison metrics will likely better identify sources of model errors and
 15 point to the directions for model improvements. Next-generation model-data comparison should
 16 evolve beyond comparing the spatial and temporal means and make more use of these
 17 observational regime-specific cloud properties.

18 **Acknowledgements**

19 We thank the JPL R&TD FY08 funding support and discussions with Drs. Joao Teixeira and
 20 Xianglei Huang. This work is conducted at the Jet Propulsion Laboratory, California Institute of
 21 Technology, under contract with NASA.

1 **References**

- 2 Back, L. E., and C. S. Bretherton (2006), Geographic variability in the export of moist static
3 energy and vertical motion profiles in the tropical Pacific, *Geophys. Res. Lett.*, **33**, L17810,
4 doi:10.1029/2006GL026672.
- 5 Bony, S., et al. (2004), On dynamic and thermodynamic components of cloud changes, *Clim.*
6 *Dyn.*, **22**, 71–86.
- 7 Emanuel, K.A. (1994), Atmospheric convection. Oxford University Press, Oxford, UK, 580pp.
- 8 Haynes J. M., and G.L. Stephens (2007), Tropical oceanic cloudiness and the incidence of
9 precipitation, *Geophys. Res. Lett.*, **34**, L09811, doi:10.1029/2007GL029335.
- 10 Johnson, R. H. et al. (1999), Trimodal characteristics of tropical convection, *J. Clim.*, **12**, 2397–
11 2418.
- 12 Klein, S. A., and D.L. Hartmann (1993), The seasonal cycle of low stratiform clouds. *J. Clim.*, **6**,
13 1587-1606, 1993.
- 14 Kubar T. L., and D. L. Hartmann (2008), Vertical structure of tropical oceanic convective clouds
15 and its relation to precipitation, *Geophys. Res. Lett.*, **35**, L03804, doi:10.1029/2007GL032811.
- 16 Lindzen, R. S., and S. Nigam (1987), On the role of sea surface temperature gradients in forcing
17 low level winds and convergence in the tropics. *J. Atmos. Sci.*, **44**, 2418-2436.
- 18 Wyant, M. C., et al. (2006), A comparison of low-latitude cloud properties and their response to
19 climate change in three AGCMs sorted into regimes using mid-tropospheric vertical velocity.
20 *Clim. Dyn.*, **27**, 261-279.
- 21 Zhang, Y., et al. (2007), Cluster analysis of tropical clouds using CloudSat data, *Geophys. Res.*
22 *Lett.*, **34**, L12813, doi:10.1029/2007GL029336.

1 **Figure Captions**

2 **Figure 1.** (a) Tropical and (b) zonal mean CWC (IWC+LWC) profiles observed by CloudSat
3 averaged for 2007.

4 **Figure 2.** Maps of the annual mean CloudSat observed CWC at four heights, (a) 16 km, (b) 9 km,
5 (c) 5 km and (d) 2 km.

6 **Figure 3.** The CloudSat observed CWC profiles sorted by eight large-scale parameters. The PDF
7 of each large-scale parameter is plotted in dashed black curve. The map of each large-scale
8 parameter is shown below the corresponding binned plot.

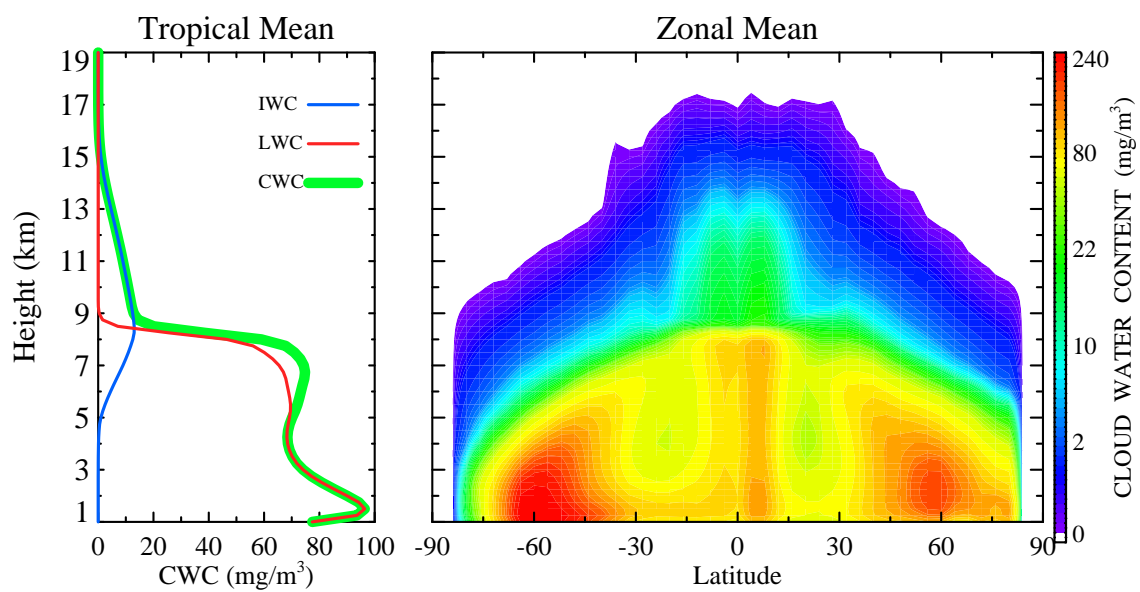


Figure 1

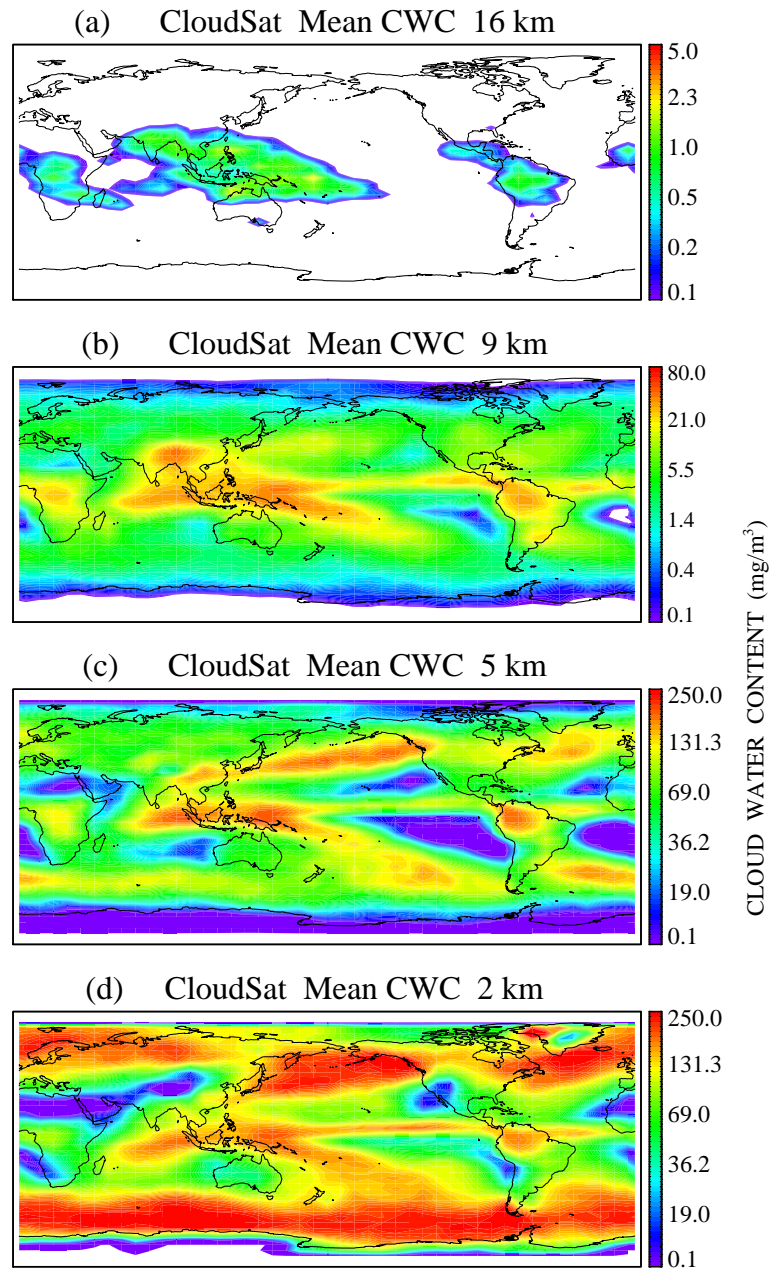


Figure 2

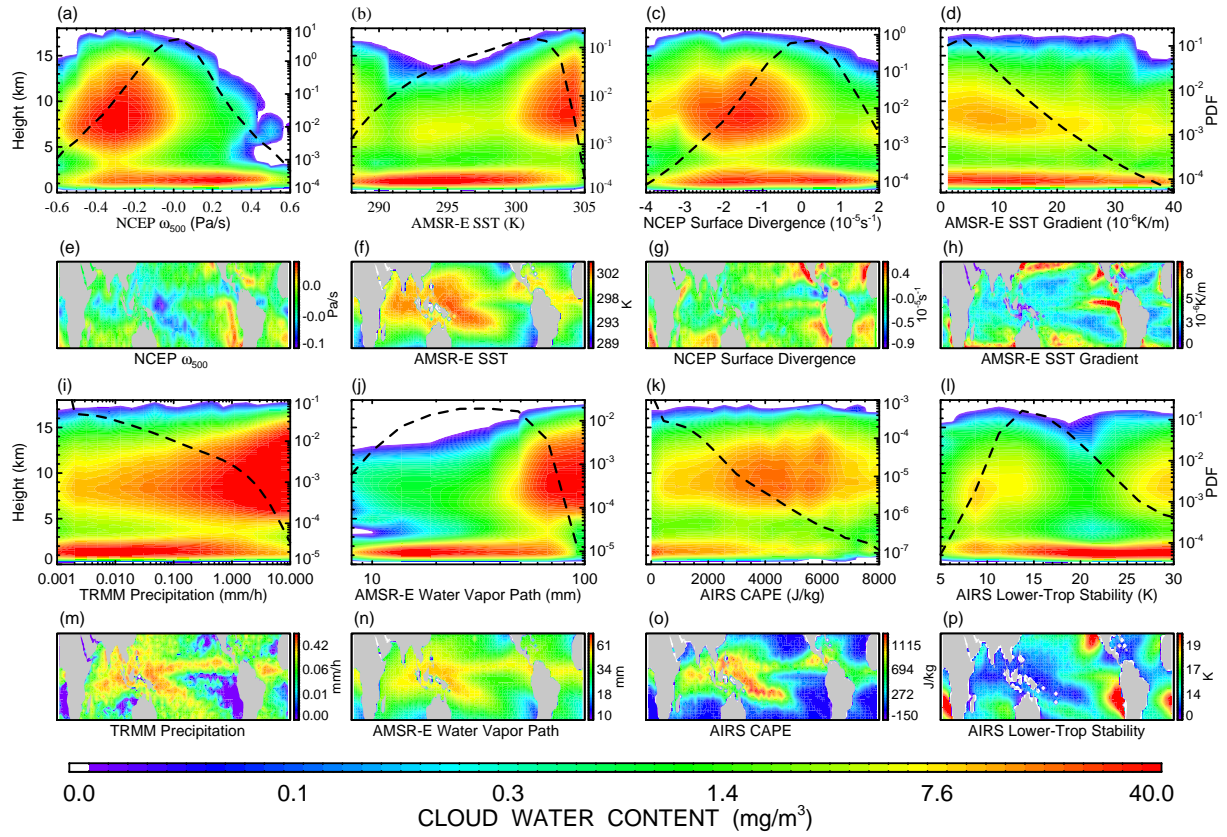


Figure 3